Journal of Water Resource and Protection, 2026, 18(8), 500-525
https://www.scirp.org/journal/jwarp
ISSN Online: 1945-3108
ISSN Print: 1945-3094

Comparative Assessment of Irrigation Water Requirements for Major Crops in the Senegal River Basin Using AgERA5 and NASA POWER Reanalysis Data

Adja Salamata Gassama[1,2*], Lamine Diop[1,2], Ousseynou Badji[1,2], Aminata Sarr[3], Ansoumana Bodian[4], Aliou Diop[5]

[1]Laboratory of Biological, Agronomic and Food Sciences and Modelling of Complex Systems (LABAAM), Gaston Berger University, Saint Louis, Senegal
[2]Faculty of Agronomic Sciences, Aquaculture and Food Technology, Gaston Berger University, Saint Louis, Senegal
[3]Renewable Energy and Energy Efficiency Laboratory, International Institute for Water and Environmental Engineering (2iE), Ouagadougou, Burkina Faso
[4]Leïdi Laboratory-Dynamics of Territories and Development, Gaston Berger University (UGB), Saint-Louis, Senegal
[5]Faculty of Applied Sciences and Technology (SAT), Gaston Berger University (UGB), Saint-Louis, Senegal
Email: *gassama.adja-salamata@ugb.edu.sn

How to cite this paper: Gassama, A.S., Diop, L., Badji, O., Sarr, A., Bodian, A. and Diop, A. (2026) Comparative Assessment of Irrigation Water Requirements for Major Crops in the Senegal River Basin Using AgERA5 and NASA POWER Reanalysis Data. *Journal of Water Resource and Protection*, **18**, 500-525.
https://doi.org/10.4236/jwarp.2026.188026

Received: July 21, 2026
Accepted: August 23, 2026
Published: August 26, 2026

Abstract

Reliable estimates of irrigation water requirements are essential for agricultural water planning in the Senegalese part of the Senegal River Basin, where rainfall variability, high evaporative demand and agricultural intensification place increasing pressure on water resources. This study evaluated AgERA5 and NASA POWER for estimating reference evapotranspiration and quantifying gross irrigation water requirements for rice with 115-day, 125-day and 150-day cycles, onion and tomato over the 1984-2025 period. Reference evapotranspiration was calculated using the FAO-56 Penman-Monteith method, and product performance was evaluated against eight ground stations located in open environments or within irrigated schemes. Both products reproduced monthly reference evapotranspiration satisfactorily at the open synoptic stations, with AgERA5 providing the estimates closest to the observations. NASA POWER showed larger deviations during the hot dry season. Overestimation was more pronounced at stations located within irrigated schemes, particularly during the dry seasons, highlighting differences in spatial representativeness between local irrigated conditions and gridded climate data. Gross irrigation water requirements ranged from 7158 $m^3 \cdot ha^{-1}$ for 115-day rice in Upper Ferlo during the rainy season with NASA POWER to 22,269 $m^3 \cdot ha^{-1}$ for 150-

day rice in the Middle Senegal Valley during the hot dry season with the same product. The effect of sowing date also varied according to crop cycle and climate product. The difference between the least and most water-demanding sowing dates ranged from 905 $m^3 \cdot ha^{-1}$ for 115-day rice during the hot dry season with AgERA5 to 3672 $m^3 \cdot ha^{-1}$ for 150-day rice during the same season with NASA POWER. Early-season sowings required less water for rainy-season rice and for onion and tomato during the cool dry season. Across all crops, seasons and management units, the mean absolute difference between AgERA5 and NASA POWER was approximately 997 $m^3 \cdot ha^{-1}$. During the rainy season, both products identified the Middle Senegal Valley as having the highest requirements and Upper Ferlo as having the lowest, whereas their spatial rankings differed more during the dry seasons. Sobol analysis showed that ET_0 was most sensitive to wind speed during the dry seasons and to relative humidity during the rainy season. These findings demonstrate that AgERA5 and NASA POWER can support regional irrigation planning in data-scarce areas, provided that spatial scale, sowing date and climate-product selection are considered.

Keywords

AgERA5, Climate Reanalysis, Irrigated Agriculture, Irrigation Water Requirements, NASA POWER, Senegal River Basin

1. Introduction

The global population is projected to reach nearly ten billion by 2050. This growth will require a substantial increase in food production, accompanied by an expansion of irrigated agriculture and its water demand [1] [2]. Irrigation plays an essential role in food security and socio-economic development, particularly in arid and semi-arid regions where it strongly supports agricultural productivity [3]. However, agriculture already accounts for more than 70% of global freshwater withdrawals [4]. Improving water-use efficiency therefore requires, among other measures, accurate estimation of crop water requirements.

This challenge is particularly important in the Sahel. In the Senegal River Basin, low and irregular rainfall severely constrains rainfed agriculture. Recurrent droughts since the 1970s have reinforced the strategic importance of water control for stabilising agricultural production [5] [6]. These constraints are compounded by the marked hydroclimatic changes observed in recent decades. Projected warming and increasing rainfall variability are expected to intensify evaporative demand and pressure on regional water resources [7]-[9]. These changes may further increase dependence on irrigation.

Estimating crop water requirements relies primarily on reference evapotranspiration, denoted ET_0. The FAO-56 Penman-Monteith method is the standard approach because it accounts for the main climatic factors controlling evapotranspiration [10]. However, its application requires complete climatic records, which are often unavailable in data-scarce regions such as the Senegal River Basin [11]. Gridded climate products derived from reanalyses, models and satellite observations offer an alternative to sparse station networks. They provide spatially continuous and temporally consistent data [12]-[15]. However, their performance varies across variables, regions and spatial resolutions. Their accuracy must therefore be assessed before use, particularly in semi-arid environments characterised by high evaporative demand [16]-[19].

In the Senegal River Basin, such assessments remain limited. Most studies have focused on estimating reference evapotranspiration without comprehensively quantifying irrigation water requirements at the basin scale [11] [20]. The few studies addressing irrigation water demand have mainly been restricted to the delta [21]. The combined effects of season, crop cycle length, sowing date and spatial variability therefore remain insufficiently documented across the Senegalese part of the basin.

This study evaluates the performance of AgERA5 and NASA POWER in estimating ET_0 using synoptic stations and stations located within irrigated perimeters. It then quantifies the gross irrigation water requirements of the major irrigated crops and analyses their variability according to season, crop cycle length, sowing date and sub-UGP. Finally, a global Sobol sensitivity analysis is applied to identify the main climatic factors controlling ET_0 variability.

2. Methods

2.1. Study Area

The study was conducted in the Senegalese part of the Senegal River Basin, located between 14˚ and 17˚N and between 13˚ and 17˚W. The Senegal River Basin is the largest and most water-abundant river basin in the country. Its Senegalese part covers approximately 76,618 km^2, representing more than one-third of the national territory [22].

The quantitative assessment of irrigation water requirements focuses on the five sub-units of the Senegal River Valley Management and Planning Unit shown in **Figure 1**. These sub-units, referred to as sub-UGP, comprise the Senegal Delta, the Middle Senegal Valley, Lower Ferlo, Thiangol-Louguéré and Upper Ferlo. They cover approximately 63,352 km^2, calculated from the spatial boundaries used in this study, and contain the main irrigated areas in the Senegalese part of the basin. The Falémé sub-unit, which drains the southeastern edge of the basin and belongs to the Eastern Senegal Management and Planning Unit, was excluded because it contains little irrigated land.

The study area is characterised by a marked south-to-north rainfall gradient. Precipitation is highest in the southeastern part of the basin and decreases towards the northern and northwestern regions, where annual totals can fall below 200 mm [23] [24]. The rainfall regime is unimodal, with precipitation mainly concentrated between June and October and a long dry season during the remainder of the year [24] [25]. Low and highly irregular rainfall constrains rainfed agriculture and reinforces the role of irrigation in agricultural production [8] [21].

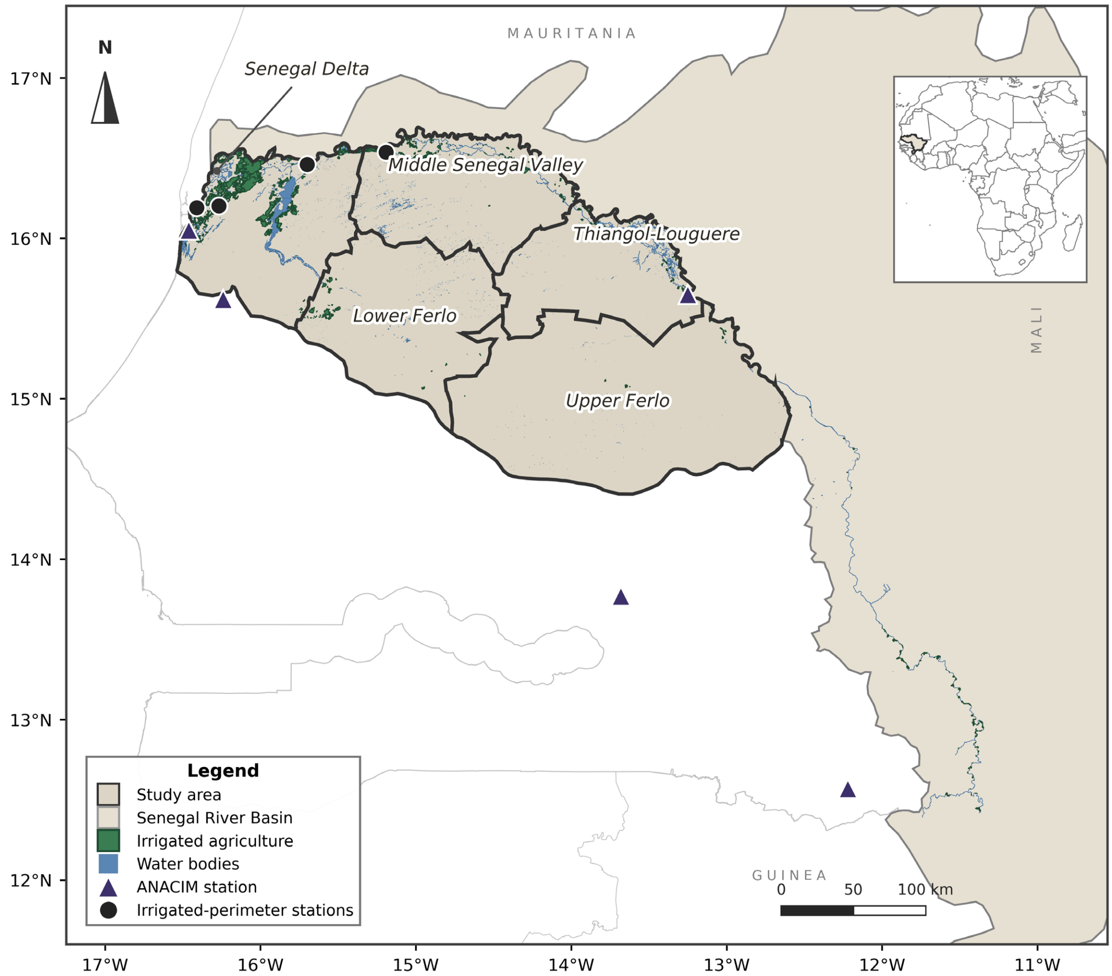

Figure 1. Location of the study area in the Senegalese part of the Senegal River Basin. The map shows the five sub-units of the Senegal River Valley Management and Planning Unit retained for the assessment of irrigation water requirements. It also shows irrigated areas, water bodies, synoptic stations operated by the National Agency for Civil Aviation and Meteorology, ANACIM, and stations located within irrigated perimeters.

2.2. Data Sources

Daily climate data covering the 1984-2025 period were obtained from two gridded climate products: AgERA5 and NASA POWER. AgERA5 is an agrometeorological dataset derived from the ERA5 reanalysis, with a spatial resolution of 0.1˚, equivalent to approximately 10 km [26]. NASA POWER meteorological data are primarily derived from the MERRA-2 reanalysis and have a spatial resolution of 0.5˚ × 0.625˚ [13] [27]. The variables used include minimum and maximum air temperature, relative humidity, wind speed, solar radiation and precipitation.

Observational data were obtained from the eight meteorological stations presented in **Table 1**. These comprise five synoptic stations operated by the National Agency for Civil Aviation and Meteorology, ANACIM, and located in open environments, as well as three stations installed within irrigated perimeters in the

Saint-Louis region. The observation periods vary among stations. Each climate product was therefore compared with observations over the station-specific common period. All variables were harmonised beforehand in accordance with the FAO-56 requirements.

Table 1. Characteristics of the ground-based meteorological stations used to evaluate reference evapotranspiration (ET_0).

Station		Lat (˚N)	Long. (˚W)	Period
ANACIM stations	Saint-Louis	16.05	16.46	1984-2021
	Louga	15.62	16.24	1984-2011
	Matam	15.65	13.25	1984-2021
	Kedougou	12.57	12.22	1984-2022
	Tambacounda	13.77	13.68	1984-2022
Irrigated-perimeter stations	Fanaye	16.54	15.19	2013-2025
	Ndiaye	16.20	16.27	2013-2025
	Diama	16.19	16.41	2018-2024

2.3. Reference Evapotranspiration (ET_0) Estimation

Reference evapotranspiration was estimated using the FAO-56 Penman-Monteith equation [10]:

$$ET_0 = \frac{0.408\Delta\left(R_n - G\right) + \gamma\left(\frac{900}{T+273}\right)U_2\left(e_s - e_a\right)}{\Delta + \gamma\left(1 + 0.34U_2\right)}. \tag{1}$$

where Δ is the slope of the saturation vapour pressure curve in kPa·˚C^{-1}, R_n is the net radiation in MJ m^{-2}·day^{-1} and G is the soil heat flux density in the same unit. T is the mean air temperature in ˚C, γ is the psychrometric constant in kPa·˚C^{-1}, U_2 is the wind speed at 2 m in m·s^{-1} and $e_s - e_a$ is the vapour pressure deficit in kPa. All parameters were calculated following the standard FAO-56 procedure [10].

AgERA5 wind speed, available at 10 m, was adjusted to 2 m using the logarithmic wind profile recommended by FAO-56. A conversion factor of 0.748 was applied. NASA POWER wind speed was directly available at 2 m.

At the daily time step, soil heat flux was assumed to be negligible and set to zero, in accordance with the FAO-56 recommendations [10]. For the monthly ET_0 calculated from the ANACIM synoptic station data and used for validation, soil heat flux was estimated from the change in monthly mean air temperature.

2.4. Effective Precipitation (P_e)

Effective precipitation was estimated using the FAO and AGLW method implemented in CROPWAT [28]:

$$\text{For } P \le 70\,\text{mm/month}. \qquad P_e = 0.6P - 10 \tag{2}$$

$$\text{For } P > 70 \text{ mm/month}. \quad P_e = 0.8P - 24 \tag{3}$$

where P_e is the monthly effective precipitation and P is the total monthly precipitation, both expressed in millimetres. Negative values of P_e were set to zero. For the calculation of irrigation water requirements, monthly effective precipitation was then distributed to the daily time step in proportion to the precipitation observed on each day. The FAO/AGLW method is defined at the monthly scale because effective precipitation represents the fraction of monthly rainfall stored in the root zone and available to the crop, a quantity that is not meaningful at the daily scale. To feed the daily requirement chain while preserving this monthly balance, the monthly effective precipitation was distributed over the days of the month in proportion to the observed daily rainfall, so that the daily values sum to the monthly effective total and follow the actual temporal distribution of rain.

2.5. Irrigation Water Requirements

Crop evapotranspiration was calculated using the following equation:

$$ET_c = ET_0 * K_c \tag{4}$$

where K_c is the crop coefficient corresponding to the crop type and growth stage. Crop coefficients for irrigated lowland rice have been determined from field measurements under semi-arid Sahelian conditions [29].

Net irrigation water requirements were calculated as follows:

$$\text{NIR} = ET_c - P_e \tag{5}$$

Net irrigation requirements were calculated at the daily time step. When effective precipitation exceeded crop evapotranspiration, the resulting negative values were set to zero before aggregation over the crop cycle, and excess effective precipitation was not carried over to subsequent days. Following the FAO-56 crop-coefficient approach, these requirements represent the water needed to meet crop evapotranspiration and do not include land preparation, initial ponding, deep percolation or drainage specific to lowland rice. These excluded components depend primarily on soil hydraulic properties, field conditions and irrigation management rather than on the climate product considered; since the study compares two climate products, restricting the requirement to its evapotranspiration-driven component avoids introducing variability unrelated to the comparison. On the heavy clay soils that dominate the delta rice areas, measured percolation is moreover modest (1.5 - 2 mm·day^{-1}; Raes *et al.* [30]). This choice is consistent with the regional assessments of Diop *et al.* [20] and Djaman *et al.* [31], and the rice requirements represent an evapotranspiration-based lower bound of the total flooded-field requirement. Gross irrigation water requirements were then calculated using the following equation:

$$\text{GIR} = \frac{\text{NIR}}{E_i} \tag{6}$$

where E_i is irrigation efficiency. Irrigation efficiency varies among schemes with the method, canal condition and management, and measured project efficiencies in the valley range from 48% to 61% [30]. In the absence of scheme-specific measured values across the study area, a single reference value of 0.70 was adopted, the default recommended by FAO for well-managed gravity irrigation [27] and consistent with the value used for the Senegal River Delta by Diop *et al.* [20]. It was applied uniformly to ensure comparability across crops, seasons and products. Because gross requirements scale inversely with efficiency, adopting the lower measured efficiencies would raise the reported values by about 15% to 46%; as a common factor applied identically to both products, the efficiency affects only the absolute level of the requirements and not the comparison between AgERA5 and NASA POWER. The cropping seasons, sowing windows and crop parameters used in the study are presented in **Table 2** and **Tables 3**.

Table 2. Cropping seasons, crops, cycle lengths and sowing windows considered in the study.

Cropping season	Crops and cycle length	Sowing window
Hot dry season	Rice with 115, 125 and 150-day cycles	1 Feb - 31 Mar
Rainy season	Rice with 115, 125 and 150-day cycles	1 Jul - 31 Aug
Cool dry season	Onion with a 120-day cycle and tomato with a 135-day cycle	1 Oct - 30 Nov

Table 3. Parameters of the main crops considered in the study.

Crop	Scientific name	Maximum root depth (m)	Length of growth stages (days)					Crop coefficient (K_c)			Growing seasons
			L_{ini}	L_{dev}	L_{mid}	L_{late}	L_{Totale}	$K_{c\,ini}$	$K_{c\,mid}$	$K_{c\,late}$	
Onion	*Allium cepa* L.	0.3 - 0.6	25	35	40	20	120	0.7	1.05	0.75	Cood dry season
Rice	*Oryza sativa* L.	0.5 - 1.0	30	35	35	15	115	1.05	1.2	0.75	Hot dry season and Rainy season
Rice	*Oryza sativa* L.	0.5 - 1.0	35	30	35	25	125	1.05	1.2	0.75	
Rice	*Oryza sativa* L.	0.5 - 1.0	30	30	60	30	150	1.05	1.2	0.75	
Tomato	*Solanum lycopersicum* L.	0.7 - 1.5	30	40	40	25	135	0.60	1.15	0.80	Cood dry season

L represents the duration of the growth stage. The subscripts ini, dev, mid and late refer to the initial, development, mid-season and late-season stages, respectively. K_c is the crop coefficient. Sources: Doorenbos and Pruitt [29], Allen *et al.* [10] and FAO [4].

2.6. Performance of Reanalysis Datasets in Estimating Reference Evapotranspiration (ET_0)

The performance of AgERA5 and NASA POWER was evaluated using eight ground stations divided into two complementary groups. Five ANACIM synoptic stations located in open environments were used for validation: Saint-Louis, Louga, Matam, Kédougou and Tambacounda. Matam was retained but analysed separately because wind speed was estimated rather than measured. Three stations located within irrigated perimeters, namely Fanaye, Ndiaye, and Diama, were used to assess the spatial representativeness of the products.

Comparisons were conducted at the monthly scale, which was the only temporal scale common to all records. At the ANACIM stations, ET_0 was calculated directly at the monthly scale using the FAO-56 Penman-Monteith method and accounting for monthly soil heat flux [10]. At Fanaye, Ndiaye and Diama, ET_0 was calculated at the daily scale from the observed meteorological variables and then aggregated into monthly means. The eight retained stations differ only in the time step of the FAO-56 computation, monthly at the ANACIM synoptic stations and daily aggregated to monthly at the three perimeter stations a difference of minor magnitude, the Penman-Monteith equation yielding similar estimates at the monthly and daily steps [10]; all reference values are computed with measured Penman-Monteith. For each climate product, daily ET_0 calculated using the FAO-56 Penman-Monteith method was extracted from the grid cell nearest to each station and then aggregated into monthly means. Estimates from the products and stations were therefore compared at the same temporal scale. For each station, the evaluation period corresponds to the common period between the available observations and the climate products. These periods are presented in **Table 1**.

Relative humidity was directly available in both products and was not derived, and solar radiation was converted to $MJ \cdot m^{-2} \cdot day^{-1}$ where required. The station records were screened with physical-range checks on each variable, and values outside plausible bounds were discarded; the Ndiaye series excludes 2019-2020 because of a humidity-sensor drift, and days with fewer than 20 hourly values were removed at Diama. The number of monthly values retained for each station and season is reported in **Table 4**. Monthly means were computed from the quality-checked daily values available in each month, and station-season combinations with fewer than five monthly values were not evaluated.

Performance was evaluated separately for each season using the root mean square error, normalised root mean square error, percent bias and Pearson correlation coefficient.

$$\mathrm{RMSE} = \sqrt{\frac{1}{n}\sum_{i=1}^{n}\left(P_i - O_i\right)^2} \tag{7}$$

$$\mathrm{NRMSE} = \frac{\mathrm{RMSE}}{\bar{O}} \times 100 \tag{8}$$

where P_i and O_i represent the ET_0 estimated from the climate product and calculated from station observations at time i, respectively. n is the number of observations and $\bar{O}$ is the mean of the station-derived values.

Percent bias was used to quantify systematic overestimation or underestimation:

$$P_{\mathrm{Biais}} = \left[\frac{\sum_{i=1}^{n}\left(P_i - O_i\right)}{\sum_{i=1}^{n} O_i}\right] \times 100 \tag{9}$$

A positive value indicates overestimation, while a negative value indicates underestimation.

The Pearson correlation coefficient measures agreement in temporal variability between the estimates and observations. It was calculated as follows:

$$r = \frac{\sum_i^n \left(O_i - \bar{O}\right)\left(P_i - \bar{P}\right)}{\sqrt{\sum_i^n \left(O_i - \bar{O}\right)^2 \sum_{i=1}^n \left(P_i - \bar{P}\right)^2}} \tag{10}$$

where $\bar{P}$ is the mean of the values estimated from the climate product.

2.7. Spatial Representation of Irrigation Water Requirements

AgERA5 estimates were mapped on their native 0.1˚ grid, which represents spatial variations within the sub-UGP. Given its resolution of 0.5˚ × 0.625˚, NASA POWER provides only a limited number of grid cells across the study area. Its estimates were therefore calculated as area-weighted zonal means for each sub-UGP. For each unit, the zonal mean was computed as a cosine-latitude-weighted average of the grid cells assigned to that unit by the management-unit mask, each cell being assigned to the unit containing its centre; basin-scale means were computed in the same way over the five units.

The two products were compared at the common spatial scale of the sub-UGP [32]-[35]. AgERA5 estimates were therefore aggregated to the same scale as NASA POWER estimates. This scale corresponds to the units used for irrigation planning and management, and errors associated with the spatial aggregation of climatic variables generally remain limited [36].

For each sub-UGP, the difference was calculated by subtracting the NASA POWER estimate from the AgERA5 estimate. Positive values therefore indicate higher requirements with AgERA5, while negative values indicate higher requirements with NASA POWER. This approach allows the two products to be compared and the spatial variability of irrigation water requirements to be analysed across sub-UGP and cropping seasons.

2.8. Sensitivity Analysis

A global sensitivity analysis was conducted using the variance-based Sobol method [37]. This method partitions the total variance of the output into the individual effects of the input variables and their interactions. It is widely used in agrohydrological modelling to identify the variables that contribute most to output variability [38]-[40]. It has been applied in particular to analyse the climatic factors controlling crop yield and crop water use [41] [42].

For a model with k input variables, the total output variance $V(Y)$ is expressed as follows:

$$V(Y) = \sum_i V_i + \sum_{i<j} V_{ij} + \cdots + V_{1,2,\cdots,k} \tag{11}$$

where V_i represents the individual contribution of variable i, V_{ij} represents the interaction between variables i and j, and $V_{1,2,\cdots,k}$ represents higher-order interactions.

The first-order index of variable i was calculated as follows:

$$\text{First order index}\left(S_i\right) = \frac{V_i}{V(Y)} \tag{12}$$

The S_i index measures the direct contribution of variable i to the output variance. The total-order index accounts for this direct contribution and all interactions involving variable i. It is expressed as follows:

$$\text{Total index}\left(S_T\right)=1-\frac{V_i}{V\left(Y\right)} \tag{13}$$

where V_i represents the contribution to variance of all terms that do not involve variable i. A small difference between S_i and S_{T_i} indicates limited interactions, whereas a large difference indicates a stronger contribution from interactions [39].

Sampling was performed using the Saltelli scheme [43], with a base sample size of 512 and the calculation of second-order indices. Three climatic variables were analysed: mean air temperature, relative humidity, wind speed and solar radiation. The daily temperature range was held at its median value. With three input variables, the sampling design required 5120 model evaluations.

For each sample, ET_0 was recalculated using the FAO-56 Penman-Monteith method. The climatic variables were sampled independently between their 5th and 95th percentiles. These limits were determined separately for each climate product, sub-UGP and cropping season. The resulting indices therefore represent ET_0 sensitivity within the range of variation specific to each climatic context.

3. Results

3.1. Performance of AgERA5 and NASA POWER in Estimating Reference Evapotranspiration

The performance of AgERA5 and NASA POWER in estimating monthly ET_0 varied according to season and station type. PBIAS, NRMSE and the correlation coefficient were calculated for each station and cropping season. Detailed results are presented in **Table 4**.

At the three synoptic stations with measured wind speed, AgERA5 generally provided the estimates closest to the observations. Its PBIAS ranged from −5% to +13% during the hot dry season, from +4% to +14% during the cool dry season and from −9% to +3% during the rainy season. NRMSE ranged from 7% to 17% across all seasons. NASA POWER showed larger deviations, particularly during the hot dry season, with PBIAS ranging from +4% to +29% and NRMSE from 13% to 31%. Its PBIAS decreased during the cool dry and rainy seasons, ranging from +4% to +17% and from −4% to +18%, respectively. Correlation coefficients varied substantially according to station and season, with neither product showing a consistent advantage. The results for Matam were considered separately because wind speed was estimated rather than measured. At this station, PBIAS ranged from +10% to +25% for AgERA5 and from +4% to +20% for NASA POWER, depending on the season. Correlations were high during the hot dry and rainy seasons but decreased markedly during the cool dry season.

At the stations located within irrigated perimeters, both products systematically overestimated observed ET_0. However, the magnitude of this overestimation varied according to station and season. During the cool dry season, PBIAS ranged from +26% to +76% for AgERA5 and from +8% to +54% for NASA POWER, with the highest values observed at Fanaye. During the hot dry season, PBIAS ranged from +19% to +40% for AgERA5 and from +17% to +41% for NASA POWER. The deviations generally decreased during the rainy season, ranging from +7% to +32% for AgERA5 and from +3% to +36% for NASA POWER.

Table 4. Performance of AgERA5 and NASA POWER in estimating monthly ET_0 by station, climate product and cropping season. Seasonal performance is reported using PBIAS, NRMSE and the correlation coefficient.

Station	Product	Hot dry season				Rainy season				Cool dry season			
		PBias %	NRMSE %	r	n	PBias %	NRMSE %	r	n	PBias %	NRMSE %	r	n
Saint-Louis	AgERA5	−5	12	0.7	179	1.3	7.9	0.22	108	8.8	13	0.43	140
Saint-Louis	NASA POWER	28.9	31.1	0.64		17.5	21.8	0.1*		17.2	19.6	0.46	
Louga	AgERA5	13.1	14.9	0.74	131	−1.6	7.4	0.69	78	13.9	16.6	0.43	103
Louga	NASA POWER	20	21.4	0.71		0.1	9.8	0.69		8.4	15.3	0.2	
Kedougou	AgERA5	2.2	12.1	0.72	182	2.8	13.8	0.35	103	3.9	12.5	0.76	133
Kedougou	NASA POWER	4.4	12.7	0.76		−3.9	15.2	0.12*		7.9	17	0.74	
Tambacounda	AgERA5	6.1	11.4	0.59	175	−9.3	11.9	0.78	104	3.8	11.2	0.75	134
Tambacounda	NASA POWER	22.5	25	0.59		−1.8	9.6	0.8		3.8	18.4	0.71	
Matam	AgERA5	17.6	18.7	0.81	190	10.2	13.2	0.84	112	24.8	26.2	0.33	150
Matam	NASA POWER	19.6	20.5	0.84		4	12	0.84		7.8	18.1	0.02*	
Fanaye	AgERA5	40.4	42.6	0.61	65	15.8	18.7	0.71	39	76	78.7	0.03*	51
Fanaye	NASA POWER	41	42.7	0.72		14.2	18.6	0.74		54	58.5	0.05*	
Ndiaye	AgERA5	27.5	32.9	0.21*	62	14.3	17.7	0.49	35	53	58.3	0.02*	47
Ndiaye	NASA POWER	18.4	24.4	0.37		4.1	12.4	0.48		29.7	38.8	0*	
Diama	AgERA5	19	21.1	0.57	29	6.7	10	0.51*	15	25.8	26.9	0.68	23
Diama	NASA POWER	17.3	18.8	0.72		3.2	12.5	0.3*		7.6	12.5	0.56	

Correlations marked with an asterisk are not significant at $p < 0.05$.

These results reveal a clear contrast between the synoptic stations located in open environments and those installed within irrigated perimeters. Both products performed satisfactorily at most synoptic stations but showed greater overestimation of ET_0 within irrigated perimeters, particularly during the dry seasons.

3.2. Seasonal Variability and Effect of Sowing Date on Irrigation Water Requirements

Gross irrigation water requirements varied with season, crop cycle length and sowing date, as shown in **Figure 2** and **Figure 3** and **Table 5**. During the hot dry season, mean basin-scale requirements for rice increased from approximately 15,800 to 19,600 m³·ha⁻¹ with AgERA5 and from 17,200 to 20,900 m³·ha⁻¹ with NASA POWER between the 115-day and 150-day cycles. For the 115-day cycle, the AgERA5 estimate was close to the reference dose of 16,000 m³·ha⁻¹, whereas the NASA POWER estimate exceeded this value. For the 125-day and 150-day cycles, estimates from both products exceeded the reference dose.

During the hot dry season, irrigation requirements generally decreased with delayed sowing. Correlation coefficients ranged from −0.74 to −0.98. The difference between the least and most water-demanding sowing dates ranged from 905 to 3672 m³·ha⁻¹, equivalent to 5.7% to 17.6% of the mean requirement. This difference increased with cycle length and was consistently larger with NASA POWER. Maximum requirements occurred for sowings conducted at the beginning of February or during its first three weeks, whereas minimum requirements occurred for sowings at the end of March.

During the rainy season, mean requirements ranged from approximately 10,000 to 13,800 m³·ha⁻¹ with AgERA5 and from 8300 to 11,900 m³·ha⁻¹ with NASA POWER. At basin scale, they remained below the reference dose of 12,000 m³·ha⁻¹, except for the 150-day cycle with AgERA5. Early-season sowings showed the lowest requirements. Delayed sowing increased irrigation requirements, with correlation coefficients ranging from +0.92 to +0.96. The amplitude of variation ranged from 1352 to 2360 m³·ha⁻¹, equivalent to 11.1% to 21.1% of the mean requirement. Minimum values occurred during the first half of July and maximum values at the end of August.

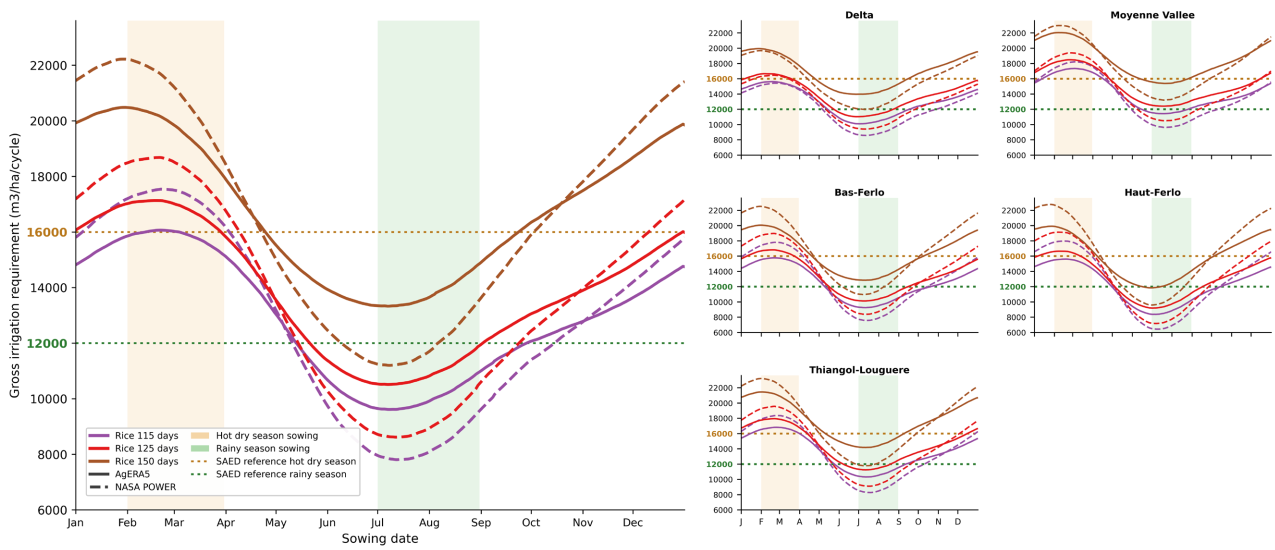

Figure 2. Variation in gross irrigation water requirements for rice according to sowing date during the hot dry and rainy seasons, at basin scale and across the five sub-UGP. Solid lines represent AgERA5 and dashed lines represent NASA POWER.

During the cool dry season, mean requirements were approximately 11,000 m³·ha⁻¹ for onion and ranged from 12,900 to 13,100 m³·ha⁻¹ for tomato. They exceeded the reference dose of 9000 $m^3 \cdot ha^{-1}$ with both products. Early-season sowings showed the lowest requirements. Delayed sowing led to an almost linear increase in irrigation requirements between 1 October and 30 November, with correlation coefficients equal to or greater than 0.999. The amplitude of variation ranged from 1411 to 2833 $m^3 \cdot ha^{-1}$, equivalent to 12.8% to 21.8% of the mean requirement.

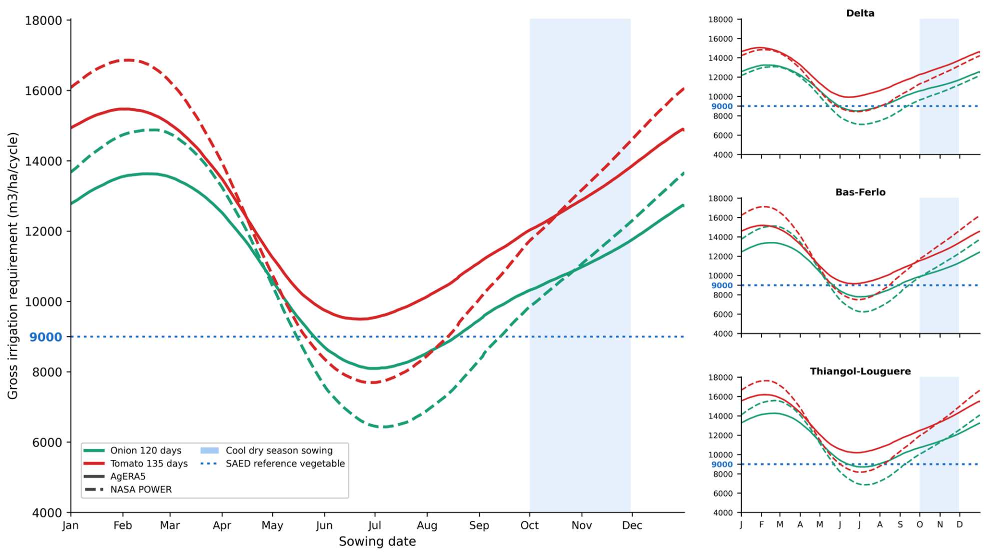

Figure 3. Variation in gross irrigation water requirements for onion and tomato according to sowing date during the cool dry season, at basin scale and across the five sub-UGP. Solid lines represent AgERA5 and dashed lines represent NASA POWER. The shaded area indicates the sowing window, and the horizontal line indicates the SAED reference dose.

Table 5. Variation in gross irrigation water requirements according to sowing date, season, crop and climate product at basin scale.

Season	Crop	Product	Mean	Min (date)	Max (date)	Δ GIR	Δ (%)	r
Hot dry	Rice 115 d	AgERA5	15,836	15,162 (31 Mar)	16,067 (21 Feb)	905	5.7	−0.78
	Rice 115 d	NASA POWER	17,210	16,240 (31 Mar)	17,539 (21 Feb)	1299	7.5	−0.74
	Rice 125 d	AgERA5	16,809	15,880 (31 Mar)	17,133 (18 Feb)	1253	7.5	−0.89
	Rice 125 d	NASA POWER	18,192	16,838 (31 Mar)	18,682 (20 Feb)	1844	10.1	−0.88
	Rice 150 d	AgERA5	19,598	17,974 (31 Mar)	20,479 (1 Feb)	2505	12.8	−0.97
	Rice 150 d	NASA POWER	20,874	18,539 (31 Mar)	22,212 (1 Feb)	3672	17.6	−0.98
Rainy	Rice 115 d	AgERA5	10,040	9613 (8 Jul)	10,965 (31 Aug)	1352	13.5	+0.95
	Rice 115 d	NASA POWER	8309	7807 (12 Jul)	9563 (31 Aug)	1756	21.1	+0.92
	Rice 125 d	AgERA5	10,947	10,511 (7 Jul)	11,912 (31 Aug)	1400	12.8	+0.96
	Rice 125 d	NASA POWER	9163	8617 (12 Jul)	10,543 (31 Aug)	1926	21.0	+0.93
	Rice 150 d	AgERA5	13,812	13,329 (7 Jul)	14,860 (31 Aug)	1530	11.1	+0.95
	Rice 150 d	NASA POWER	11,948	11,200 (8 Jul)	13,560 (31 Aug)	2360	19.8	+0.96
Cool dry	Onion 120 d	AgERA5	10,983	10,320 (1 Oct)	11,731 (30 Nov)	1411	12.8	+0.999
	Onion 120 d	NASA POWER	11,040	9853 (1 Oct)	12,259 (30 Nov)	2406	21.8	+1.000
	Tomato 135 d	AgERA5	12,879	12,030 (1 Oct)	13,825 (30 Nov)	1794	13.9	+0.999
	Tomato 135 d	NASA POWER	13,125	11,728 (1 Oct)	14,561 (30 Nov)	2833	21.6	+1.000

Across all sub-UGP, crops and seasons, irrigation water requirements ranged from 7158 to 22,269 $m^3 \cdot ha^{-1}$. At basin scale, NASA POWER provided higher estimates during the hot dry season, whereas AgERA5 produced higher values during the rainy season. Depending on the crop and season, the effect of sowing date was comparable to or greater than the difference between the two products. The amplitude associated with sowing date was consistently larger with NASA POWER.

3.3. Spatial Variability of Irrigation Water Requirements

Irrigation water requirements computed with AgERA5 are represented on its native 0.1˚ grid, whereas NASA POWER estimates are aggregated across the five sub-UGP. The spatial distributions obtained for the different cropping seasons are presented in Figures 4-6.

During the hot dry season, irrigation requirements increase with crop cycle length in all sub-UGP. With AgERA5, they range from 15,295 - 17,148 $m^3 \cdot ha^{-1}$ for the 115-day cycle to 18,682 - 21,549 $m^3 \cdot ha^{-1}$ for the 150-day cycle. With NASA POWER, the corresponding ranges increase from 15,196 - 18,054 to 18,764 - 22,269 $m^3 \cdot ha^{-1}$. For both products, the requirements of the 125-day cycle lie between those of the other two cycles.

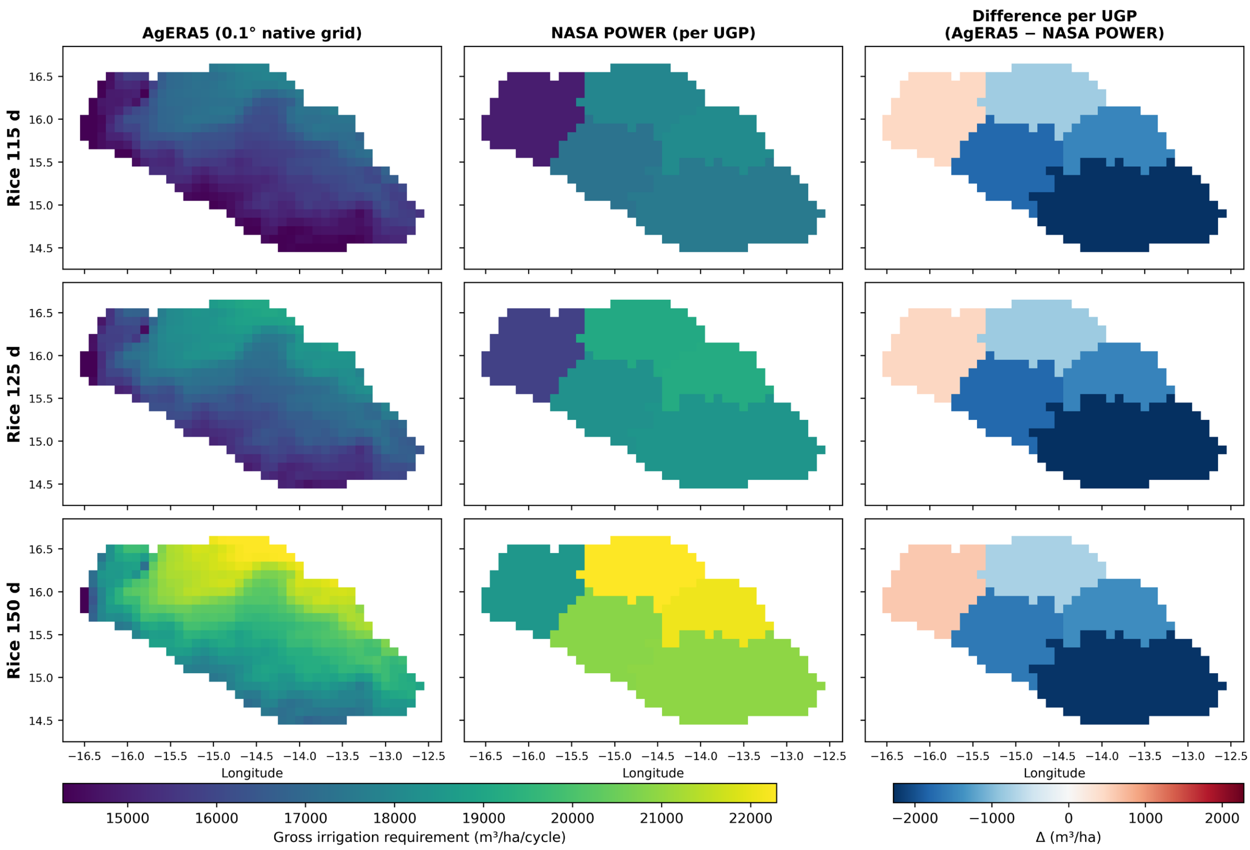

Figure 4. Spatial distribution of gross irrigation water requirements for rice during the hot dry season for the 115-day, 125-day and 150-day cycles. The first column presents AgERA5 estimates on the native 0.1˚ grid. The second presents NASA POWER estimates aggregated by sub-UGP. The third presents the difference between AgERA5 and NASA POWER.

The highest requirements are mainly observed in the Middle Senegal Valley and Thiangol-Louguéré. The lowest values occur in Upper Ferlo with AgERA5 and in the Senegal Delta with NASA POWER. NASA POWER provides higher estimates than AgERA5 in all sub-UGP except the Delta. The mean difference, calculated as AgERA5 minus NASA POWER, ranges from +244 $m^3 \cdot ha^{-1}$ in the Delta to −2125 $m^3 \cdot ha^{-1}$ in Upper Ferlo. The location of the maximum depends on the cycle length and climate product. For the 115-day and 125-day cycles, AgERA5 places the maximum in the Middle Senegal Valley, whereas NASA POWER places it in Thiangol-Louguéré. For the 150-day cycle, both products place the maximum in the Middle Senegal Valley.

During the rainy season, irrigation requirements are markedly lower but also increase with crop cycle length. With AgERA5, they range from 8989 - 11,616 $m^3 \cdot ha^{-1}$ for the 115-day cycle to 12,649 - 15,583 m^3 $m \cdot ha^{-1}$ for the 150-day cycle. With NASA POWER, the corresponding ranges increase from 7158 - 9876 to 10,811 - 13,547 $m^3 \cdot ha^{-1}$. AgERA5 provides higher estimates than NASA POWER in all sub-UGP, with mean differences ranging from 1523 to 2044 $m^3 \cdot ha^{-1}$. Despite this systematic difference, both products produce the same spatial ranking for all three cycles. The highest requirements occur in the Middle Senegal Valley and the lowest in Upper Ferlo.

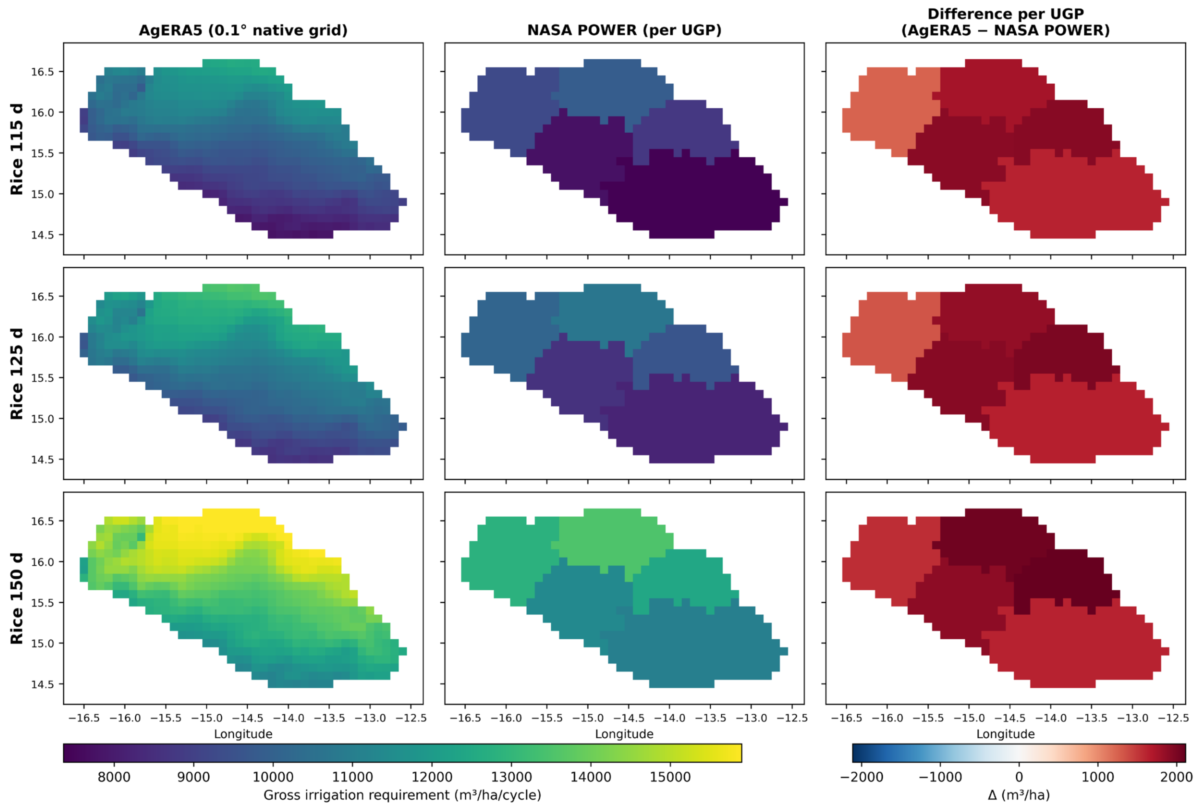

Figure 5. Spatial distribution of gross irrigation water requirements for rice during the rainy season for the 115-day, 125-day and 150-day cycles. The first column presents AgERA5 estimates on the native 0.1˚ grid. The second presents NASA POWER estimates aggregated by sub-UGP. The third presents the difference between AgERA5 and NASA POWER.

During the cool dry season, differences among the sub-UGP are less pronounced. Onion requirements range from 10,543 to 11,456 $m^3 \cdot ha^{-1}$ with AgERA5 and from 10,388 to 11,351 $m^3 \cdot ha^{-1}$ with NASA POWER. Tomato requirements range from 12,386 to 13,409 $m^3 \cdot ha^{-1}$ and from 12,214 to 13,573 $m^3 \cdot ha^{-1}$, respectively.

The two products provide similar estimates of the overall level of irrigation requirements, but their spatial distributions differ. AgERA5 produces higher values in the Delta and the Middle Senegal Valley, whereas NASA POWER provides higher estimates in Lower and Upper Ferlo. With AgERA5, the maximum occurs in the Middle Senegal Valley and the minimum in Lower Ferlo. With NASA POWER, the maximum occurs in Upper Ferlo and the minimum in the Delta.

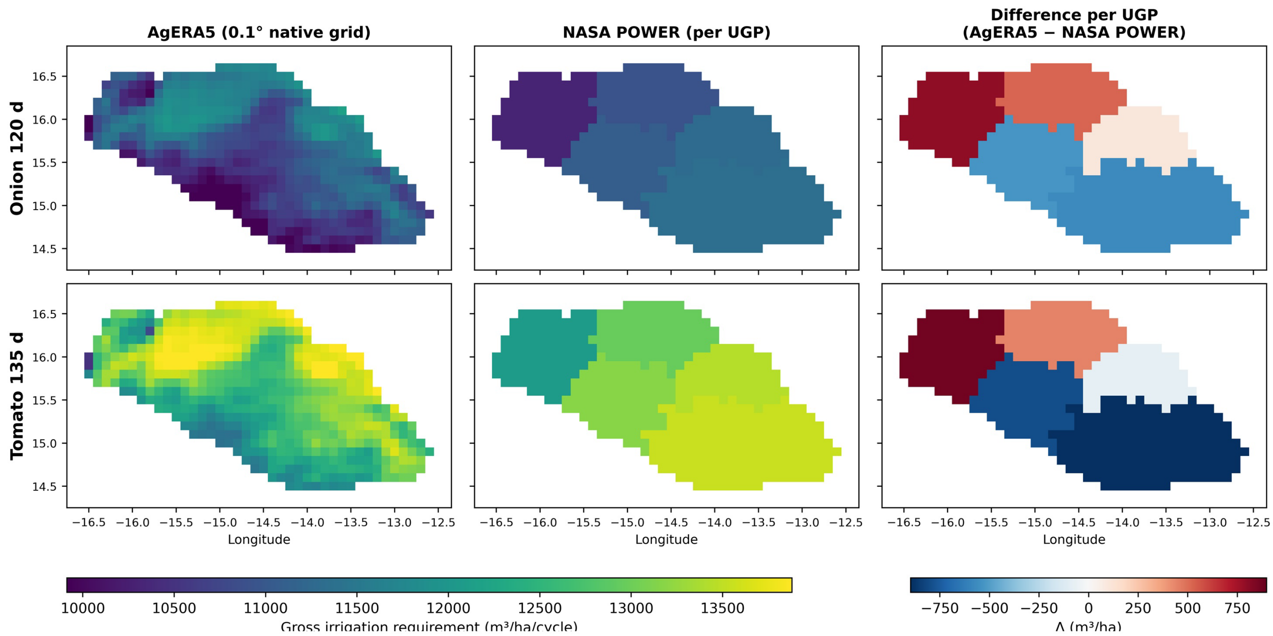

Figure 6. Spatial distribution of gross irrigation water requirements for onion and tomato during the cool dry season. The first column presents AgERA5 estimates on the native 0.1˚ grid. The second presents NASA POWER estimates aggregated by sub-UGP. The third presents the difference between AgERA5 and NASA POWER.

Overall, the intensity of spatial variability depends on the season. The range among the sub-UGP represents approximately 48% of the mean requirement during the rainy season, compared with 17% during the hot dry season and 10% during the cool dry season. The mean absolute difference between AgERA5 and NASA POWER is approximately 997 $m^3 \cdot ha^{-1}$, equivalent to 7% of the mean requirement. Both products therefore reproduce the same spatial contrasts during the rainy season, whereas the ranking of the sub-UGP is less consistent during the dry seasons. The mechanisms underlying these variations and the effects of spatial resolution are examined in the Discussion.

3.4. Sensitivity Analysis of Reference Evapotranspiration

The sensitivity analysis quantified the contribution of each climatic variable to

ET_0 variability and assessed the importance of interactions according to season and climate product. The results are presented in Figure 7.

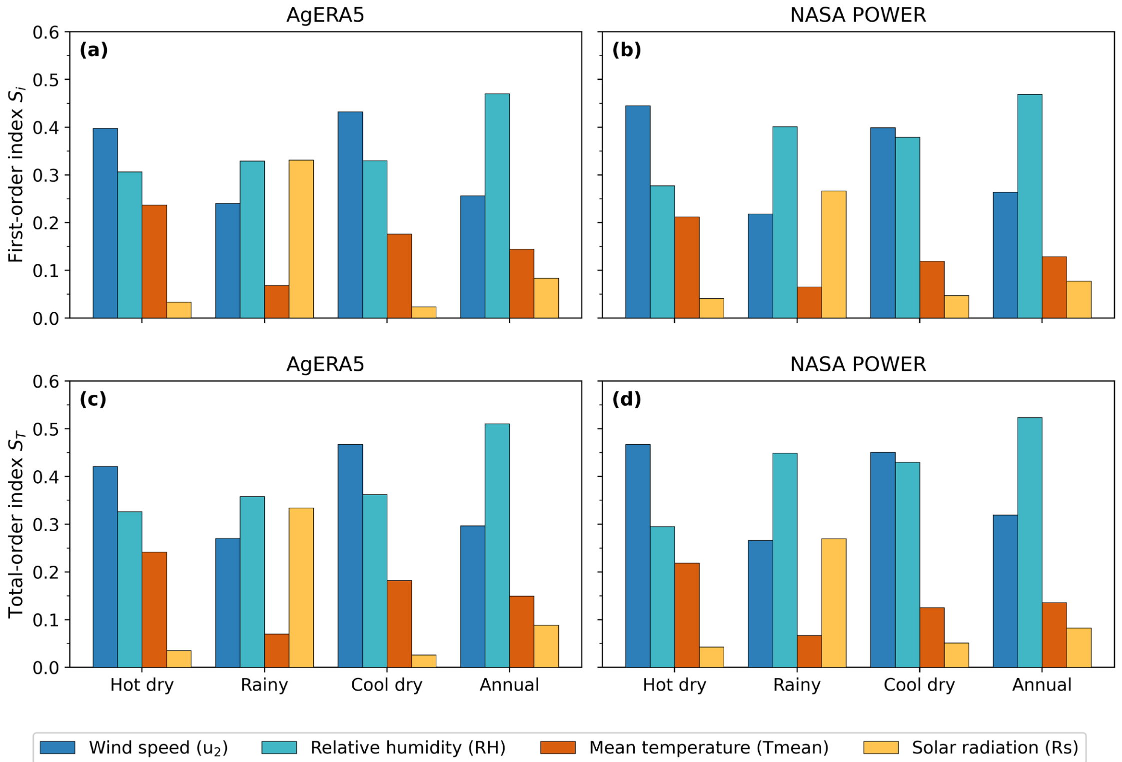

Figure 7. Sobol sensitivity indices of reference evapotranspiration to wind speed (u_2), relative humidity (RH), mean air temperature (Tmean) and incoming solar radiation (Rs) by season and climate product. Panels (a) and (b) present the first-order indices (S_i), and panels (c) and (d) the total-order indices (ST). Panels (a) and (c) correspond to AgERA5, and panels (b) and (d) to NASA POWER. Values are averaged across the five sub-UGP.

The direct effects of the three climatic variables jointly explain between 94% and 98% of the total variability in ET_0. Interactions among these variables therefore account for only the remaining 2% to 6%. Their limited contribution is also confirmed by the similarity between the first-order and total-order indices, which differ by no more than 0.06. During both dry seasons, wind speed is the main factor controlling ET_0 variability, with a mean index of 0.42. During the hot dry season, it is followed by relative humidity with an index of 0.29, mean air temperature with 0.22 and solar radiation with 0.04. A similar hierarchy is observed during the cool dry season, with indices of 0.35 for relative humidity, 0.15 for mean air temperature and 0.04 for solar radiation.

The hierarchy changes during the rainy season. Relative humidity becomes the main factor, with a mean index of 0.37, followed by solar radiation with 0.30. The contribution of wind speed decreases to 0.23, whereas that of mean air temperature remains low at 0.07. At the annual scale, relative humidity remains the main factor controlling ET_0 variability, with an index of 0.47. It is followed by wind speed with 0.26, mean air temperature with 0.14 and solar radiation with 0.08.

The two products show the same ranking of factors during the dry seasons and at the annual scale. However, a difference appears during the rainy season. With NASA POWER, relative humidity dominates solar radiation, with respective indices of 0.40 and 0.27. With AgERA5, the two variables make equal contributions, with an index of 0.33 each. Both products therefore show that the importance of wind speed decreases during the rainy season. During this season, relative humidity becomes the main factor with NASA POWER, whereas relative humidity and solar radiation contribute equally with AgERA5.

4. Discussion

4.1. Performance of AgERA5 and NASA POWER in Estimating ET_0

At the synoptic stations located in open environments, AgERA5 and NASA POWER reproduce monthly ET_0 satisfactorily overall. AgERA5 provides the estimates closest to the observations, with small seasonal biases and NRMSE values between 10% and 13%. The larger deviations observed with NASA POWER during the hot dry season may be related to its coarser spatial resolution and to the representation of the atmospheric variables used in the Penman-Monteith equation. Nevertheless, both products show their smallest biases and normalised errors during the rainy season.

The lowest, and in several cases non-significant, correlation coefficients are obtained in the cool dry season, and at some stations in the rainy season. This does not necessarily indicate poorer accuracy. The limited month-to-month variability of ET_0 in these seasons reduces the ability of the correlation coefficient to capture temporal variations, so that a weak or non-significant correlation may partly reflect the limited temporal variability of ET_0 and the available sample size and should not, on its own, be interpreted as evidence of poor product performance. PBIAS and NRMSE are therefore more appropriate for evaluating performance in these seasons.

Deviations are markedly larger at stations located within irrigated perimeters, particularly during the dry seasons. This contrast with the synoptic stations is consistent with an oasis effect. Irrigation locally maintains cooler and more humid conditions than those in the surrounding areas. Stations located within irrigated perimeters may therefore record lower evaporative demand than that represented by the climate-product grid cell, which reflects regional conditions [44] [45]. The reduction in deviations during the rainy season supports this interpretation because the contrast between irrigated areas and their surroundings becomes less pronounced. However, the oasis effect cannot explain all the observed deviations. Differences between point measurements and gridded estimates may also arise from spatial resolution, the distance between a station and the centre of the corresponding grid cell, and uncertainties in wind speed [31], relative humidity and solar radiation. These variables directly influence ET_0 estimated using the Penman-Monteith method [10]. Previous studies have also shown that the performance of gridded climate products may decline in semi-arid environments and during periods of high evaporative demand [16] [17] [19] [46].

The performance obtained at the synoptic stations indicates that AgERA5 and NASA POWER can complement observational networks in regional analyses of ET_0. The finer resolution of AgERA5 allows spatial variations within the sub-UGP to be represented in greater detail, although finer resolution alone does not guarantee higher accuracy at the local scale. For operational irrigation scheduling at the local or field scale, both products should be evaluated against observations representative of the intended scale of application. Bias correction or local calibration may be required where substantial deviations occur.

4.2. Spatio-Temporal Variability of Requirements and Implications for Irrigation Planning

Irrigation water requirements depend on the season, the cycle length, the sowing date and the location. The highest values are observed during the hot dry season, particularly for the 150-day rice cycle, because of the high evaporative demand and the small contribution of effective precipitation. The increase in requirements with cycle length is consistent with the FAO-56 approach, since cumulative requirements depend on crop evapotranspiration over the whole cycle [10]. During this season, requirements generally decrease as sowing is delayed. This decrease does not, however, always correspond to an achievable saving, because late sowings extend the cycle towards the rainy season and may encroach on the following campaign. When only the cycles completed before the start of that campaign are retained, the minimum requirements increase by 690 to 1660 $m^3 \cdot ha^{-1}$ for the 115- and 125-day cycles; for the 150-day cycle, only sowing on 1 February satisfies this constraint. In the rainy season the relationship is reversed: early-season sowings show the lowest requirements, whereas delayed sowing shifts an increasing part of the cycle beyond the wettest period. Early sowings therefore make better use of rainfall and may also limit the exposure of the sensitive phases of rice to the low temperatures of the end of the season, which affect spikelet fertility and yield; in the Senegal River valley, an appropriate choice of sowing date has been shown to avoid severe cold sterility [45].

For onion and tomato grown during the cool dry season, requirements increase almost linearly with delayed sowing. Sowings carried out early in the season benefit from a lower evaporative demand, whereas late sowings shift an increasing part of the cycle towards the hot dry season. The estimates exceed both reference values available for the valley: the planning dose used by SAED is 9000 $m^3 \cdot ha^{-1}$, whereas the theoretical requirements retained by OMVS reach 7030 $m^3 \cdot ha^{-1}$ for onion and 7200 $m^3 \cdot ha^{-1}$ for tomato [47]. This comparison must nevertheless remain cautious, as these values may rest on different definitions of the requirement and of irrigation efficiency. The project efficiencies measured in thirteen schemes of the delta and the valley, ranging from 48 to 61% [30], are all below the value of 0.70 adopted here; this assumption therefore tends to lower rather than raise the computed gross requirements. The observed differences are thus not sufficient to demonstrate that the applied doses are insufficient. Any revision would require a comparison with the volumes actually delivered, the irrigation practices and the yields obtained.

The relative spatial variability of requirements is more marked during the rainy season than during the dry seasons. This contrast is consistent with the Sahelian rainfall regime, characterised by a strong spatial heterogeneity of rainfall totals [48]. This heterogeneity, which propagates directly to effective precipitation, also tends to increase: the share of annual totals contributed by extreme events rose from 17% over 1970-1990 to 21% over 2001-2010, while the number of rainy days declined [49]. During the dry seasons, the contribution of rainfall becomes marginal and requirements depend mainly on evaporative demand, whose variations between sub-UGP are less pronounced. In the rainy season, the spatial range represents about 48% of the mean requirement, against a mean absolute difference of about 7% between AgERA5 and NASA POWER. The spatial signal then dominates the inter-product disagreement and both products give the same ranking, with higher requirements in the Middle Senegal Valley than in Upper Ferlo. In the hot dry and cool dry seasons, the spatial range falls to 17% and 10% respectively, and the differences between products become large enough to change the location of the maximum requirements.

Spatial resolution also contributes to the representation of these contrasts. AgERA5 resolves variations within the sub-UGP, whereas NASA POWER provides a more aggregated representation. The aggregation of climatic variables can influence the outputs of agronomic models, particularly where precipitation is spatially heterogeneous [32] [34] [35]. These results show that irrigation planning must take season, crop, cycle length, sowing date and sub-UGP jointly into account. The gradient common to both products during the rainy season can support the distribution of volumes between management units. During the dry seasons, the spatial ranking depends more on the climate product and should not be used on its own to prioritise allocations; a single dose per season and per crop, with a margin covering the difference between products, is then a more defensible basis than a spatial differentiation that the data do not support.

4.3. Climatic Factors Controlling ET_0

The Sobol analysis identifies two distinct seasonal regimes. During the dry seasons, wind speed is the main factor influencing ET_0 variability, followed by relative humidity and mean air temperature. This hierarchy is consistent with the important role of the aerodynamic term of the Penman-Monteith equation in dry and windy environments [10] [18] [50]-[52]. It also agrees with the global synthesis of McVicar *et al.* [53], which shows that near-surface wind speed largely governs the aerodynamic component of evaporative demand and thereby contributes to variations in reference evapotranspiration.

The hierarchy changes during the rainy season. Relative humidity becomes the main factor, while the contribution of solar radiation increases. With AgERA5, these two variables have comparable importance. This change may be associated with the more humid conditions of the monsoon. Variations in relative humidity directly affect the vapour pressure deficit and may therefore exert a greater influence on ET_0. At the same time, variability in cloud cover increases the contribution of incoming solar radiation. This result agrees with sensitivity analyses that identify relative humidity as one of the main variables influencing ET_0 [54]. At the annual scale, ET_0 is most sensitive to relative humidity, followed by wind speed, mean air temperature and solar radiation. The two products therefore show a comparable hierarchy during the dry seasons and at the annual scale. Their main difference occurs during the rainy season. NASA POWER assigns a greater contribution to relative humidity, whereas AgERA5 assigns comparable importance to relative humidity and solar radiation.

The similarity between the first-order and total-order indices indicates that interactions among the variables contribute little to the calculated variability of ET_0. This interpretation should nevertheless remain cautious because the classical Sobol analysis assumes that the input variables are independent [55], whereas climatic variables are naturally correlated. The results therefore identify the variables to which ET_0 is most sensitive but do not account for the correlations among these variables under actual climatic conditions.

4.4. Practical Implications and Scope of Application

This study provides an integrated assessment of ET_0 and irrigation water requirements across the Senegalese part of the Senegal River Basin. Three findings are particularly relevant to regional planning. Irrigation requirements depend strongly on season and crop cycle length, their variation within a given season is sensitive to sowing date, and their spatial distribution depends on the climate product when contrasts among the sub-UGP are small. The agreement between AgERA5 and NASA POWER on the seasonal hierarchy and the main spatial gradient observed during the rainy season supports the robustness of these findings. Their divergence in some sub-UGP during the dry seasons provides an indication of the sensitivity of the estimates to the choice of climate product.

These results can support cropping-season planning and the allocation of water volumes at the sub-UGP scale. They show that irrigation doses should be adjusted according to season, crop and cycle length. They also highlight the potential benefits of early-season sowing during the rainy and cool dry seasons, provided that agronomic constraints are respected. AgERA5 provides a detailed representation of spatial variations, whereas NASA POWER provides estimates that can be interpreted directly at the management-unit scale. The joint use of both products therefore helps identify robust findings and the situations in which the choice of climate data has a greater influence on the estimated water volumes.

The operational scope of these estimates remains linked to their regional scale. Irrigation efficiency and crop coefficients were applied consistently throughout the study area to ensure comparability across crops, seasons and sub-UGP. Applying the results to daily irrigation scheduling at the field scale would require local data on delivered water volumes, irrigation-system performance, cropping practices and cultivated varieties. Strengthening the observation network would also allow the products to be evaluated in sub-UGP that are currently sparsely monitored. Such data would extend the proposed regional framework towards operational recommendations adapted to local conditions.

5. Conclusions

This study evaluated AgERA5 and NASA POWER for estimating ET_0 and quantifying gross irrigation water requirements in the Senegalese part of the Senegal River Basin. Both products reproduce monthly ET_0 satisfactorily overall at synoptic stations located in open environments, with AgERA5 providing the estimates closest to the observations. The larger deviations observed within irrigated perimeters highlight the importance of spatial representativeness when comparing point measurements with gridded climate products. Estimated requirements range from 7158 to 22,269 $m^3 \cdot ha^{-1}$ depending on crop, season, cycle length and sub-UGP. Sowing date produces variations ranging from 5.7% to 21.8% of the mean seasonal requirement. Early-season sowings have the lowest requirements during the rainy and cool dry seasons, whereas the decrease associated with delayed sowing during the hot dry season remains constrained by the feasibility of the cropping calendar.

The two products provide the same spatial ranking during the rainy season, whereas the location of maximum requirements varies more during the dry seasons. Under the adopted sampling conditions, the sensitivity analysis indicates that ET_0 is most sensitive to wind speed during the dry seasons and to relative humidity during the rainy season and at the annual scale. These findings highlight the importance of considering season, crop, cycle length, sowing date and climate product when estimating irrigation water requirements. AgERA5 and NASA POWER can support regional irrigation planning in areas where observations are limited. Their joint use helps distinguish patterns reproduced by both products from results that are more sensitive to the climate data used. Application to daily irrigation scheduling at the field scale would nevertheless require additional local data on delivered water volumes, cropping practices and irrigation-system performance.

Acknowledgements

We sincerely thank all the individuals and institutions that contributed to this research. The authors gratefully acknowledge the institutions and meteorological services that provided access to observational data used in this study. We also thank the developers of the AgERA5 and NASA POWER datasets for making their data publicly available.

Author Contributions

Conceptualization, A.S.G. and L.D.; methodology, A.S.G. and L.D.; validation, L.D.; data curation, A.S.G.; writing—original draft preparation, A.S.G.; writing—

review and editing, L.D., A.S.G., O.B., A.S., A.B. and A.D. All authors have read and agreed to the published version of the manuscript.

Conflicts of Interest

The authors declare no conflicts of interest regarding the publication of this paper.

References

[1] Alexandratos, N. and Bruinsma, J. (2012) World Agriculture towards 2030/2050: The 2012 Revision. ESA Working Paper No. 12-03. FAO.

[2] Siebert, S., Kummu, M., Porkka, M., Döll, P., Ramankutty, N. and Scanlon, B.R. (2015) A Global Data Set of the Extent of Irrigated Land from 1900 to 2005. *Hydrology and Earth System Sciences*, **19**, 1521-1545. https://doi.org/10.5194/hess-19-1521-2015

[3] Hanjra, M.A. and Qureshi, M.E. (2010) Global Water Crisis and Future Food Security in an Era of Climate Change. *Food Policy*, **35**, 365-377. https://doi.org/10.1016/j.foodpol.2010.05.006

[4] FAO (2022) World Food and Agriculture: Statistical Yearbook 2022. FAO. https://doi.org/10.4060/cc2211en

[5] Hubert, P., Bader, J.C. and Bendjoudi, H. (2007) Un siècle de débits annuels du fleuve Sénégal. *Hydrological Sciences Journal*, **52**, 68-73. https://doi.org/10.1623/hysj.52.1.68

[6] Faye, C. (2013) Évaluation et Gestion Intégrée des Ressources en Eau dans un Contexte de Variabilité Hydroclimatique: Cas du Bassin Versant de la Falémé. Ph.D. Thesis, Cheikh Anta Diop University (UCAD).

[7] Sylla, M.B., Faye, A., Giorgi, F., Diedhiou, A. and Kunstmann, H. (2018) Projected Heat Stress under 1.5 °C and 2 °C Global Warming Scenarios Creates Unprecedented Discomfort for Humans in West Africa. *Earth's Future*, **6**, 1029-1044. https://doi.org/10.1029/2018ef000873

[8] Sultan, B., Defrance, D. and Iizumi, T. (2019) Evidence of Crop Production Losses in West Africa Due to Historical Global Warming in Two Crop Models. *Scientific Reports*, **9**, Article No. 12834. https://doi.org/10.1038/s41598-019-49167-0

[9] Bichet, A. and Diedhiou, A. (2018) West African Sahel Has Become Wetter during the Last 30 Years, but Dry Spells Are Shorter and More Frequent. *Climate Research*, **75**, 155-162. https://doi.org/10.3354/cr01515

[10] Allen, R.G., Pereira, L.S., Raes, D. and Smith, M. (1998) Crop Evapotranspiration: Guidelines for Computing Crop Water Requirements. FAO Irrigation and Drainage Paper No. 56, FAO.

[11] Ndiaye, P.M., Bodian, A., Diop, L., Deme, A., Dezetter, A. and Djaman, K. (2020) Evaluation and Calibration of Alternative Methods for Estimating Reference Evapotranspiration in the Senegal River Basin. *Hydrology*, **7**, Article 24. https://doi.org/10.3390/hydrology7020024

[12] Hersbach, H., Bell, B., Berrisford, P., Hirahara, S., Horányi, A., Muñoz-Sabater, J., *et al.* (2020) The ERA5 Global Reanalysis. *Quarterly Journal of the Royal Meteorological Society*, **146**, 1999-2049. https://doi.org/10.1002/qj.3803

[13] Sparks, A.H. (2018) Nasapower: A NASA POWER Global Meteorology, Surface Solar Energy and Climatology Data Client for R. *Journal of Open Source Software*, **3**, Article 1035. https://doi.org/10.21105/joss.01035

[14] Albergel, C., Dutra, E., Munier, S., Calvet, J., Munoz-Sabater, J., de Rosnay, P., *et al.* (2018) ERA-5 and ERA-Interim Driven ISBA Land Surface Model Simulations: Which One Performs Better? *Hydrology and Earth System Sciences*, **22**, 3515-3532. https://doi.org/10.5194/hess-22-3515-2018

[15] Gleixner, S., Demissie, T. and Diro, G.T. (2020) Did ERA5 Improve Temperature and Precipitation Reanalysis over East Africa? *Atmosphere*, **11**, Article 996. https://doi.org/10.3390/atmos11090996

[16] Nouri, M. and Homaee, M. (2022) Reference Crop Evapotranspiration for Data-Sparse Regions Using Reanalysis Products. *Agricultural Water Management*, **262**, Article ID: 107319. https://doi.org/10.1016/j.agwat.2021.107319

[17] Sawadogo, W., Bliefernicht, J., Fersch, B., Salack, S., Guug, S., Diallo, B., *et al.* (2023) Hourly Global Horizontal Irradiance over West Africa: A Case Study of One-Year Satellite- and Reanalysis-Derived Estimates vs. *in Situ* Measurements. *Renewable Energy*, **216**, Article ID: 119066. https://doi.org/10.1016/j.renene.2023.119066

[18] Ippolito, M., De Caro, D., Cannarozzo, M., Provenzano, G. and Ciraolo, G. (2024) Evaluation of Daily Crop Reference Evapotranspiration and Sensitivity Analysis of FAO Penman-Monteith Equation Using ERA5-Land Reanalysis Database in Sicily, Italy. *Agricultural Water Management*, **295**, Article ID: 108732. https://doi.org/10.1016/j.agwat.2024.108732

[19] Ndiaye, P.M. (2021) Évaluation, Calibration et Analyse des Tendances Actuelles et Futures de l'Évapotranspiration de Référence dans le Bassin du Fleuve Sénégal. Ph.D. Thesis, Gaston Berger University (UGB).

[20] Diop, L., Gassama, A.S., Sarr, A., Bodian, A., Ogilvie, A. and Yaseen, Z.M. (2023) A Comprehensive Assessment for Agriculture Water Requirement Main Crops of the Senegal River Delta. *Theoretical and Applied Climatology*, **155**, 2871-2883. https://doi.org/10.1007/s00704-023-04798-2

[21] USAID (2021) Senegal Water Resources Profile. Water Resources Profile Series, Sustainable Water Partnership, Winrock International.

[22] Biasutti, M. (2019) Rainfall Trends in the African Sahel: Characteristics, Processes, and Causes. *WIREs Climate Change*, **10**, e591. https://doi.org/10.1002/wcc.591

[23] Nicholson, S.E. (2013) The West African Sahel: A Review of Recent Studies on the Rainfall Regime and Its Interannual Variability. *ISRN Meteorology*, **2013**, Article ID: 453521. https://doi.org/10.1155/2013/453521

[24] Ndiaye, A., Mbaye, M.L., Arnault, J., Camara, M. and Lawin, A.E. (2023) Characterization of Extreme Rainfall and River Discharge over the Senegal River Basin from 1982 to 2021. *Hydrology*, **10**, Article 204. https://doi.org/10.3390/hydrology10100204

[25] Boogaard, H., Schubert, J., De Wit, A., Lazebnik, J., Hutjes, R. and Van der Grijn, G. (2020) Agrometeorological Indicators from 1979 to Present Derived from Reanalysis. Copernicus Climate Change Service (C3S) Climate Data Store (CDS). https://doi.org/10.24381/cds.6c68c9bb

[26] Gelaro, R., McCarty, W., Suárez, M.J., Todling, R., Molod, A., Takacs, L., *et al.* (2017) The Modern-Era Retrospective Analysis for Research and Applications, Version 2 (MERRA-2). *Journal of Climate*, **30**, 5419-5454. https://doi.org/10.1175/jcli-d-16-0758.1

[27] Smith, M. (1992) CROPWAT: A Computer Program for Irrigation Planning and Management. FAO Irrigation and Drainage Paper No. 46, FAO.

[28] Djaman, K., Rudnick, D.R., Moukoumbi, Y.D., Sow, A. and Irmak, S. (2019) Actual Evapotranspiration and Crop Coefficients of Irrigated Lowland Rice (*Oryza sativa* L.) under Semiarid Climate. *Italian Journal of Agronomy*, **14**, 1059. https://doi.org/10.4081/ija.2019.1059

[29] Doorenbos, J. and Pruitt, W.O. (1977) Guidelines for Predicting Crop Water Requirements. FAO Irrigation and Drainage Paper No. 24, FAO.

[30] Raes, D., Sy, B. and Feyen, J. (1995) Water Use in Rice Schemes in the Senegal River Delta and Valley. *Irrigation and Drainage Systems*, **9**, 117-128. https://doi.org/10.1007/bf00881671

[31] Djaman, K., Mel, V.C., Balde, A.B., Bado, B.V., Manneh, B., Diop, L., *et al.* (2016) Evapotranspiration, Irrigation Water Requirement, and Water Productivity of Rice (*Oryza sativa* L.) in the Sahelian Environment. *Paddy and Water Environment*, **15**, 469-482. https://doi.org/10.1007/s10333-016-0564-9

[32] Tustison, B., Harris, D. and Foufoula-Georgiou, E. (2001) Scale Issues in Verification of Precipitation Forecasts. *Journal of Geophysical Research*: *Atmospheres*, **106**, 11775-11784. https://doi.org/10.1029/2001jd900066

[33] Satgé, F., *et al.* (2020) Evaluation of 23 Gridded Precipitation Datasets across West Africa. *Journal of Hydrology*, **581**, Article ID: 124412. https://doi.org/10.1016/j.jhydrol.2019.124412

[34] Gampe, D. and Ludwig, R. (2017) Evaluation of Gridded Precipitation Data Products for Hydrological Applications in Complex Topography. *Hydrology*, **4**, Article 53. https://doi.org/10.3390/hydrology4040053

[35] Hoffmann, H., Zhao, G., Asseng, S., Bindi, M., Biernath, C., Constantin, J., *et al.* (2016) Impact of Spatial Soil and Climate Input Data Aggregation on Regional Yield Simulations. *PLOS ONE*, **11**, e0151782. https://doi.org/10.1371/journal.pone.0151782

[36] Sobol, I.M. (2001) Global Sensitivity Indices for Nonlinear Mathematical Models and Their Monte Carlo Estimates. *Mathematics and Computers in Simulation*, **55**, 271-280. https://doi.org/10.1016/s0378-4754(00)00270-6

[37] Razavi, S. and Gupta, H.V. (2015) What Do We Mean by Sensitivity Analysis? The Need for Comprehensive Characterization of "Global" Sensitivity in Earth and Environmental Systems Models. *Water Resources Research*, **51**, 3070-3092. https://doi.org/10.1002/2014wr016527

[38] Pianosi, F., Beven, K., Freer, J., Hall, J.W., Rougier, J., Stephenson, D.B., *et al.* (2016) Sensitivity Analysis of Environmental Models: A Systematic Review with Practical Workflow. *Environmental Modelling & Software*, **79**, 214-232. https://doi.org/10.1016/j.envsoft.2016.02.008

[39] Xu, Q., Li, J., Liang, H., Ding, Z., Shi, X., Chen, Y., *et al.* (2022) Coupling Life Cycle Assessment and Global Sensitivity Analysis to Evaluate the Uncertainty and Key Processes Associated with Carbon Footprint of Rice Production in Eastern China. *Frontiers in Plant Science*, **13**, Article 990105. https://doi.org/10.3389/fpls.2022.990105

[40] Lu, Y., Chibarabada, T.P., McCabe, M.F., De Lannoy, G.J.M. and Sheffield, J. (2021) Global Sensitivity Analysis of Crop Yield and Transpiration from the FAO-AquaCrop Model for Dryland Environments. *Field Crops Research*, **269**, Article ID: 108182. https://doi.org/10.1016/j.fcr.2021.108182

[41] Xu, Y., Albalawneh, A., Al-Zoubi, M. and Baroud, H. (2025) Variance-Based Sensitivity Analysis of Climate Variability Impact on Crop Yield Using Machine Learning: A Case Study in Jordan. *Agricultural Water Management*, **313**, Article ID: 109409. https://doi.org/10.1016/j.agwat.2025.109409

[42] Saltelli, A. (2002) Making Best Use of Model Evaluations to Compute Sensitivity Indices. *Computer Physics Communications*, **145**, 280-297. https://doi.org/10.1016/s0010-4655(02)00280-1

[43] Hao, X., Li, W. and Deng, H. (2016) The Oasis Effect and Summer Temperature Rise in Arid Regions—Case Study in Tarim Basin. *Scientific Reports*, **6**, Article No. 35418. https://doi.org/10.1038/srep35418

[44] Potchter, O., Goldman, D., Iluz, D. and Kadish, D. (2012) The Climatic Effect of a Manmade Oasis during Winter Season in a Hyper Arid Zone: The Case of Southern Israel. *Journal of Arid Environments*, **87**, 231-242. https://doi.org/10.1016/j.jaridenv.2012.07.005

[45] Wever, N. (2012) Quantifying Trends in Surface Roughness and the Effect on Surface Wind Speed Observations. *Journal of Geophysical Research*: *Atmospheres*, **117**, D11104. https://doi.org/10.1029/2011jd017118

[46] van Oort, P.A.J., Balde, A., Diagne, M., Dingkuhn, M., Manneh, B., Muller, B., *et al.* (2016) Intensification of an Irrigated Rice System in Senegal: Crop Rotations, Climate Risks, Sowing Dates and Varietal Adaptation Options. *European Journal of Agronomy*, **80**, 168-181. https://doi.org/10.1016/j.eja.2016.06.012

[47] Bonneau, M. (2001) Besoins en Eau de l'Agriculture Irriguée et de l'Agriculture de Décrue dans la Vallée du Fleuve Sénégal. Programme d'Optimisation de la Gestion des Réservoirs, Phase III, Organisation pour la Mise en Valeur du Fleuve Sénégal (OMVS) and IRD, Dakar.

[48] Ali, A. and Lebel, T. (2008) The Sahelian Standardized Rainfall Index Revisited. *International Journal of Climatology*, **29**, 1705-1714. https://doi.org/10.1002/joc.1832

[49] Panthou, G., Vischel, T. and Lebel, T. (2014) Recent Trends in the Regime of Extreme Rainfall in the Central Sahel. *International Journal of Climatology*, **34**, 3998-4006. https://doi.org/10.1002/joc.3984

[50] Yong, S.L.S., Ng, J.L., Huang, Y.F., Ang, C.K., Mirzaei, M. and Ahmed, A.N. (2023) Local and Global Sensitivity Analysis and Its Contributing Factors in Reference Crop Evapotranspiration. *Water Supply*, **23**, 1672-1683. https://doi.org/10.2166/ws.2023.086

[51] Ndiaye, P.M., Bodian, A., Diop, L., Deme, A., Dezetter, A., Djaman, K., *et al.* (2020) Trend and Sensitivity Analysis of Reference Evapotranspiration in the Senegal River Basin Using NASA Meteorological Data. *Water*, **12**, Article 1957. https://doi.org/10.3390/w12071957

[52] Pelosi, A., Terribile, F., D'Urso, G. and Chirico, G. (2020) Comparison of Era5-Land and UERRA MESCAN-SURFEX Reanalysis Data with Spatially Interpolated Weather Observations for the Regional Assessment of Reference Evapotranspiration. *Water*, **12**, Article 1669. https://doi.org/10.3390/w12061669

[53] McVicar, T.R., Roderick, M.L., Donohue, R.J., Li, L.T., Van Niel, T.G., Thomas, A., *et al.* (2012) Global Review and Synthesis of Trends in Observed Terrestrial Near-Surface Wind Speeds: Implications for Evaporation. *Journal of Hydrology*, **416**, 182-205. https://doi.org/10.1016/j.jhydrol.2011.10.024

[54] Vicente-Serrano, S.M., Azorin-Molina, C., Sanchez-Lorenzo, A., Revuelto, J., Morán-Tejeda, E., López-Moreno, J.I., *et al.* (2014) Sensitivity of Reference Evapotranspiration to Changes in Meteorological Parameters in s Pain (1961-2011). *Water Resources Research*, **50**, 8458-8480. https://doi.org/10.1002/2014wr015427

[55] Iooss, B. and Lemaître, P. (2015) A Review on Global Sensitivity Analysis Methods. In: Dellino, G. and Meloni, C., Eds., *Uncertainty Management in Simulation-Optimization of Complex Systems*, Springer, 101-122. https://doi.org/10.1007/978-1-4899-7547-8_5